

## Elucidating the Structural Dynamics of Carbon Dot Dispersed in Different Solvents and Its Red Fluorescence

Saptarshi Mandal<sup>1,2</sup>, Shakkira Erimban<sup>2</sup>, Subhrajeet Banerjee<sup>2</sup>, Snehasis Daschakraborty<sup>2,\*</sup>,  
Prolay Das<sup>2,\*</sup>

<sup>1</sup>Department of Biomedical Engineering, University of Kentucky, Lexington, USA-40536

<sup>2</sup>Department of Chemistry, Indian Institute of Technology Patna, Bihta, India-801103

\*Corresponding Authors: Prolay Das: [prolay@iitp.ac.in](mailto:prolay@iitp.ac.in); Snehasis Daschakraborty: [snehasis@iitp.ac.in](mailto:snehasis@iitp.ac.in)

### 1.1. Reagents and Materials

Alizarin red S, Glucose, p-phenylenediamine, citric acid, ethylenediamine, dimethylformamide (DMF), formamide, dimethyl sulfoxide (DMSO), sodium hydroxide, hydrochloric acid, were purchased from either Central Drug House Pvt. Ltd., India or Sisco Research Laboratories Pvt. Ltd., India. Potassium bromide, deuterated DMSO (DMSO-D6), heavy water (D<sub>2</sub>O), dialysis membrane (molecular weight cut off 2 kDa), and silicon wafers were bought from Sigma. Carbon-coated copper TEM grids (300 mesh) were obtained from Ted Pella Inc. Triple distilled water was used as the solvent unless specified.

### 1.2. Preparation of NaBH<sub>4</sub> treated CD<sub>ARS-G</sub> samples for FTIR study

200 µL V dispersion of CD<sub>ARS-G</sub> in water was treated with NaBH<sub>4</sub> (10µL, 500mM). The reaction mixture was kept for 2 h with occasional stirring. Then excess NaBH<sub>4</sub> and its by-products were removed by dialyzing (MWCO 2kDa) the mixture overnight. The dialyzed dispersion was dried using a vacuum concentrator (Eppendorf) for further studies.

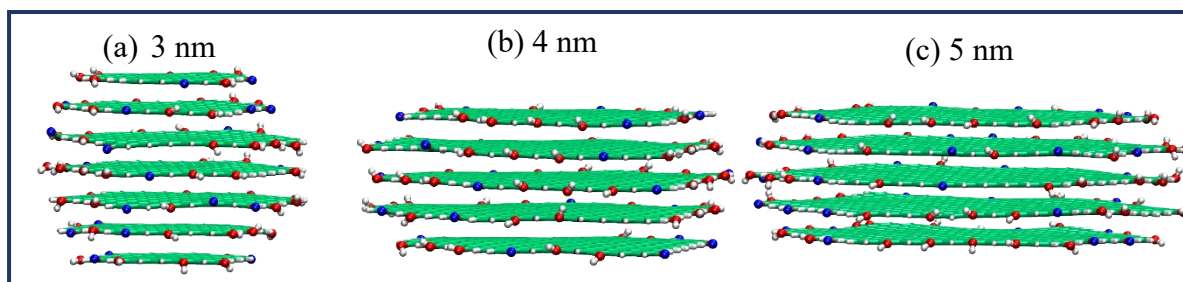


**Figure S1.** Graphical representation of the three different sized 3:7 CO: OH, CDs modeled in the simulation. Different atoms are color coded as carbon (lime green), hydroxyl oxygen (red), carbonyl oxygen (blue), and hydrogen (white).

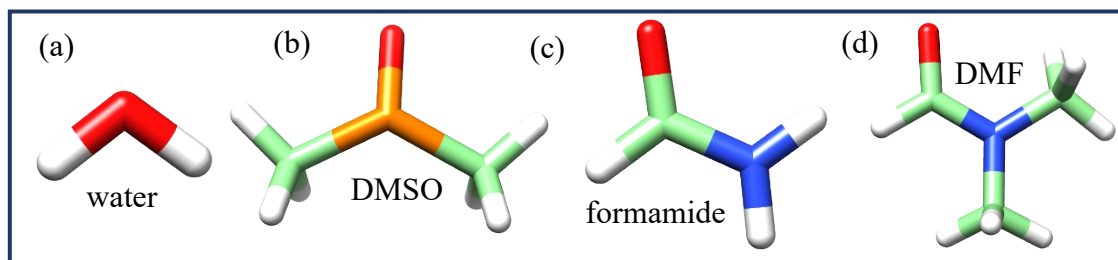


**Figure S2.** Graphical representation of four different solvent molecules considered in simulations. Different atoms are color coded as carbon (lime green), oxygen (red), hydrogen (white), nitrogen (blue) sulfur (orange).

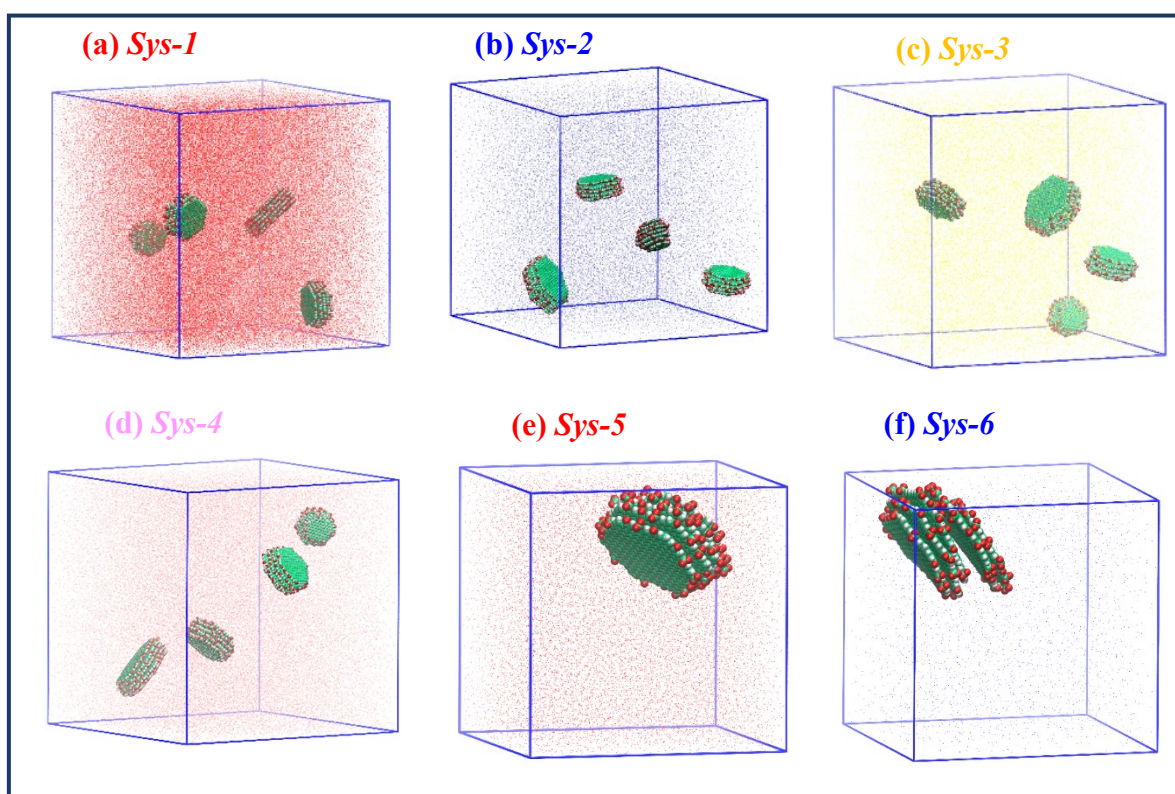


**Figure S3.** Equilibrated snapshots of the six systems after 100 ns NPT simulation runs. Different solvent systems are represented with characteristic atoms such as oxygen (red) for water, nitrogen (blue) for DMF, sulfur (yellow) for DMSO, and nitrogen (pink) for formamide. CD is shown with carbon atoms color coded with green, hydroxyl oxygen with red, carbonyl oxygen with blue, and hydrogen with white.

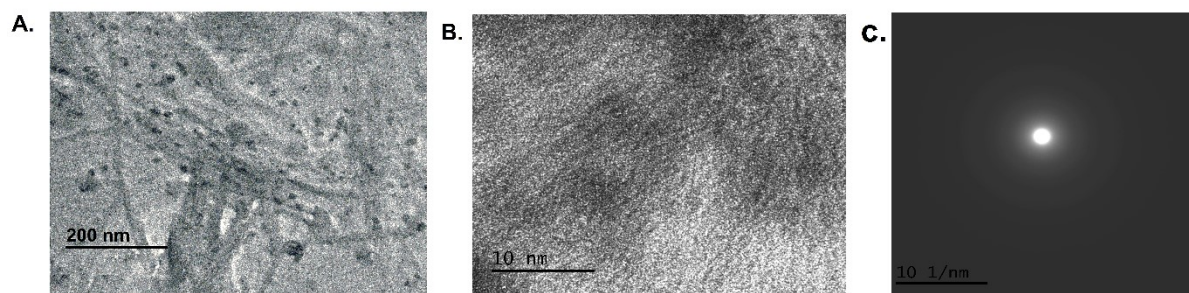


Figure S4. A. TEM, B. HR-TEM, and C. SAED pattern of CD<sub>ARS-G</sub>.

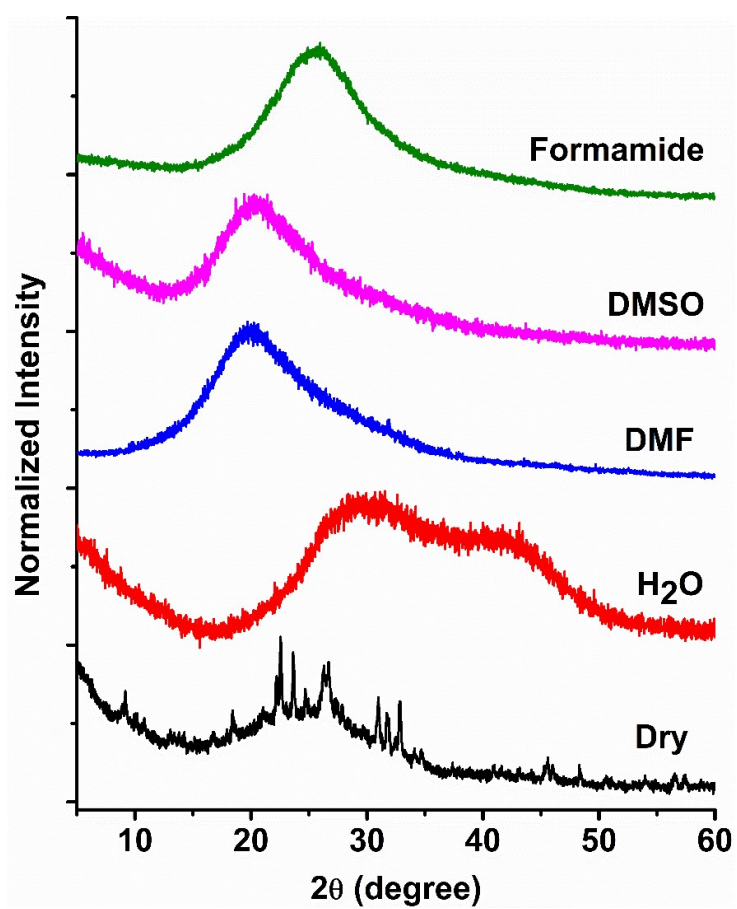


Figure S5. pXRD spectra of CD<sub>ARS-CA</sub>.

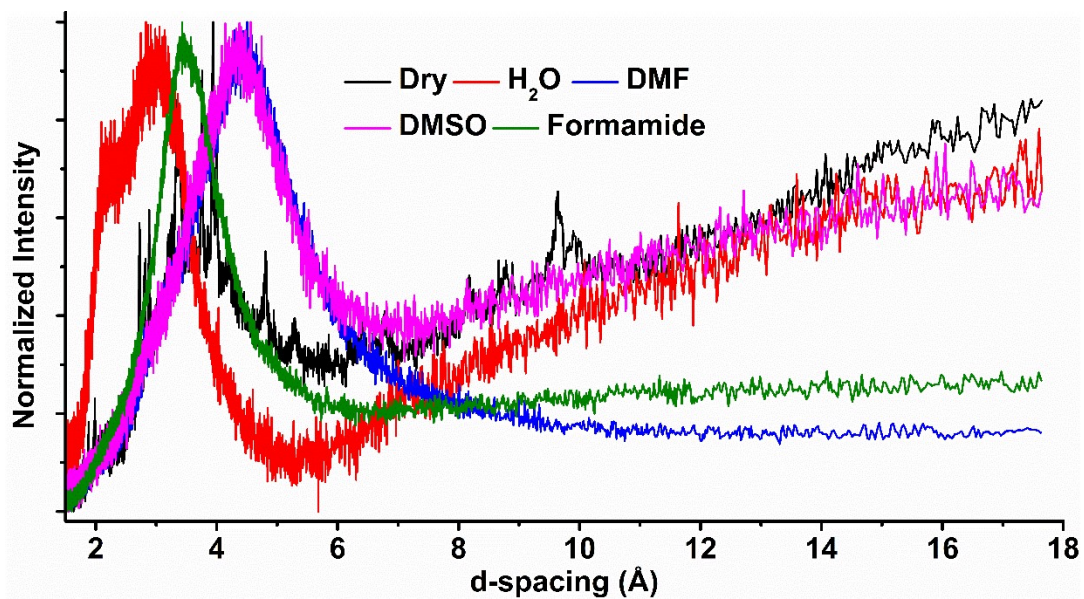


Figure S6. pXRD spectra of CD<sub>ARS-CA</sub> with respect to d-spacing values.

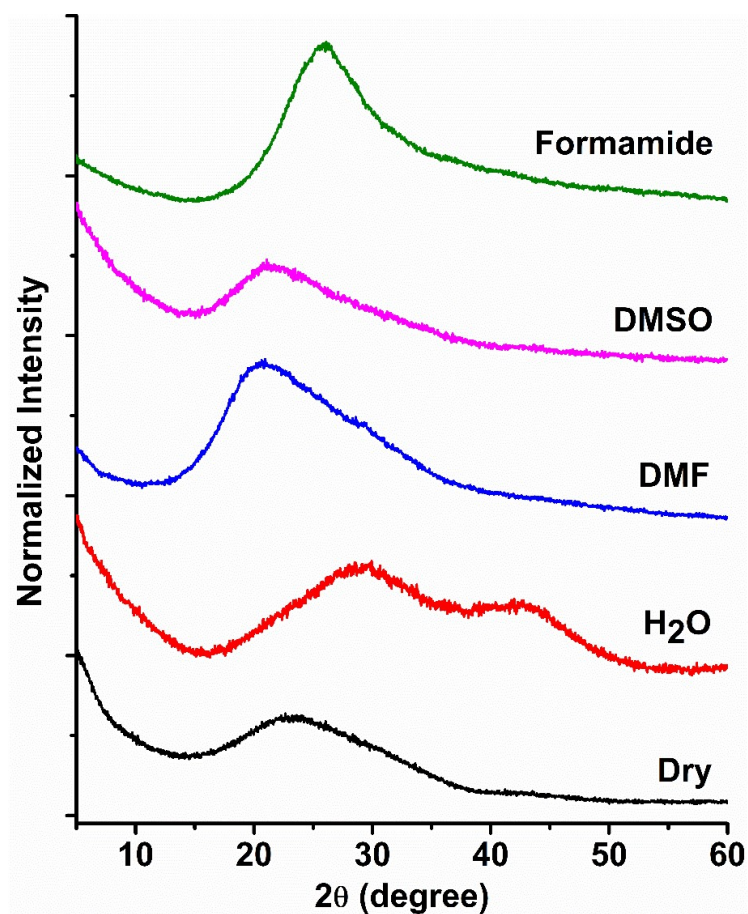


Figure S7. pXRD spectra of CD<sub>G-EDA</sub>.

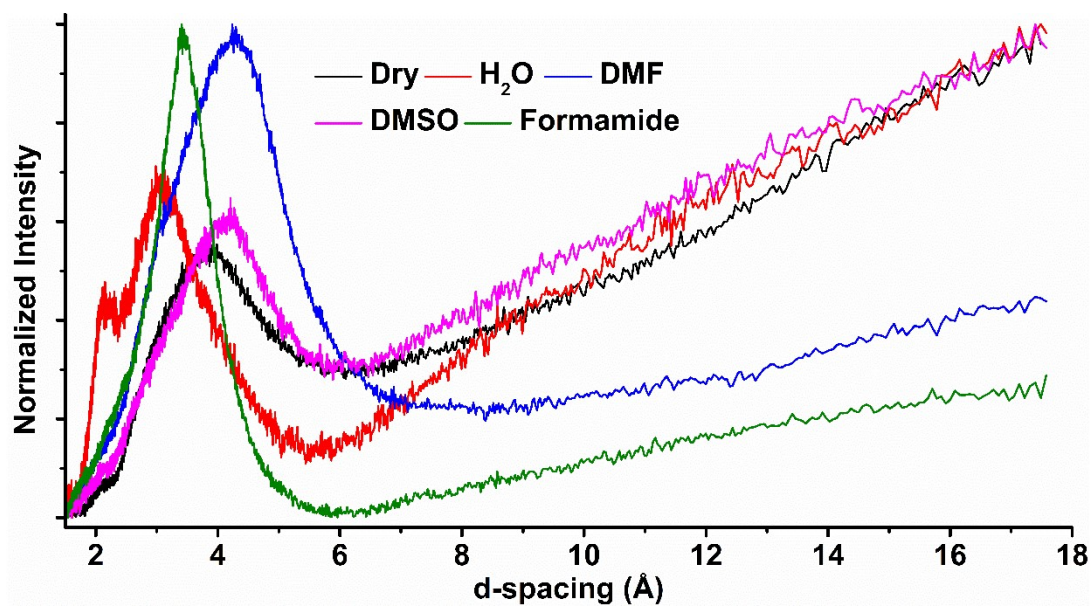


Figure S8. pXRD spectra of  $CD_{G-EDA}$  with respect to d-spacing values.

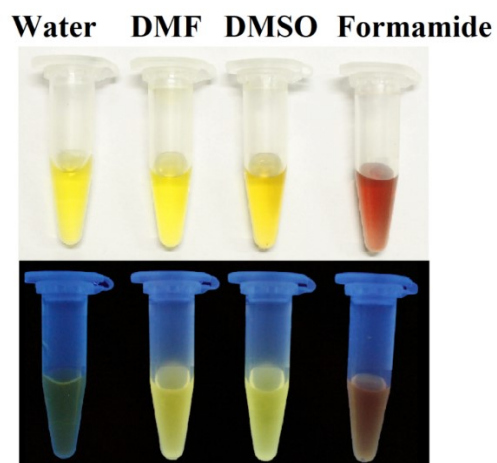
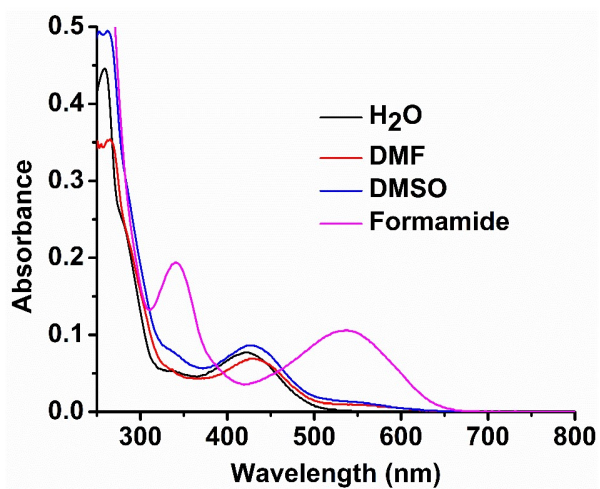
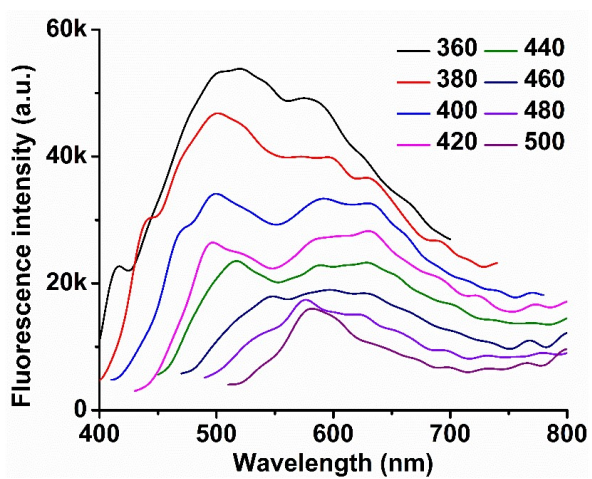


Figure S9. Digital image of  $CD_{ARS-CA}$  in water, DMF, DMSO and formamide.



**Figure S10.** UV-Vis absorption spectra of  $CD_{ARS-CA}$  in water, DMF, DMSO and formamide.



**Figure S11.** Steady-state fluorescence spectra of  $CD_{ARS-CA}$  in water.

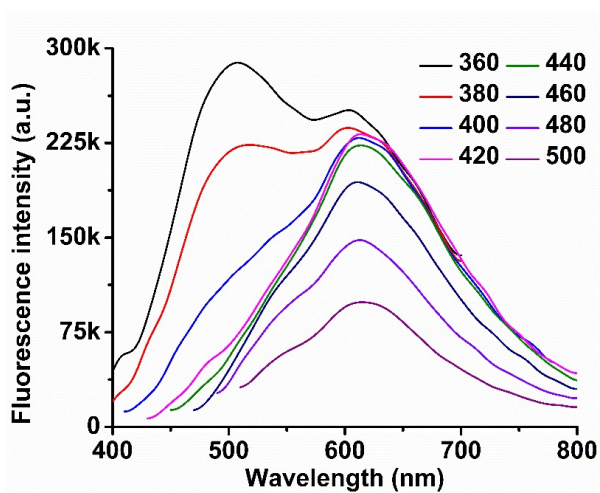


**Figure S12.** Steady-state fluorescence spectra of  $CD_{ARS-CA}$  in DMF.

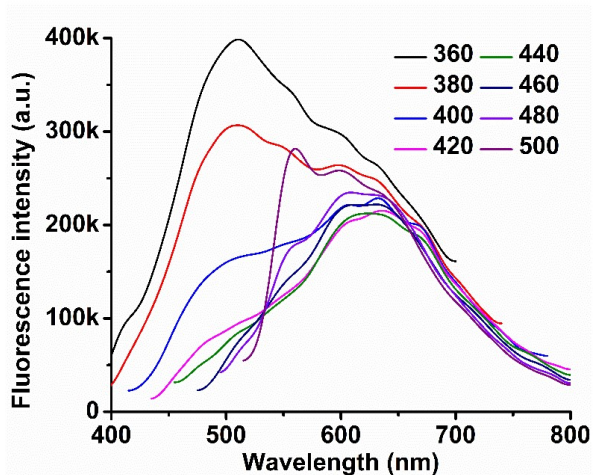


Figure S13. Steady-state fluorescence spectra of  $CD_{ARS-CA}$  in DMSO.

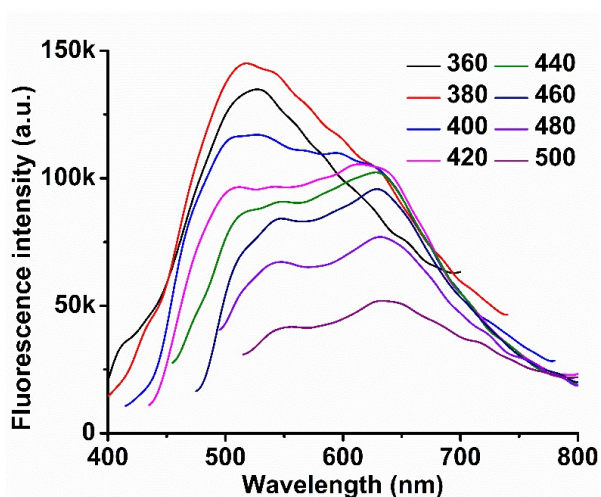


Figure S14. Steady-state fluorescence spectra of  $CD_{ARS-CA}$  in formamide.

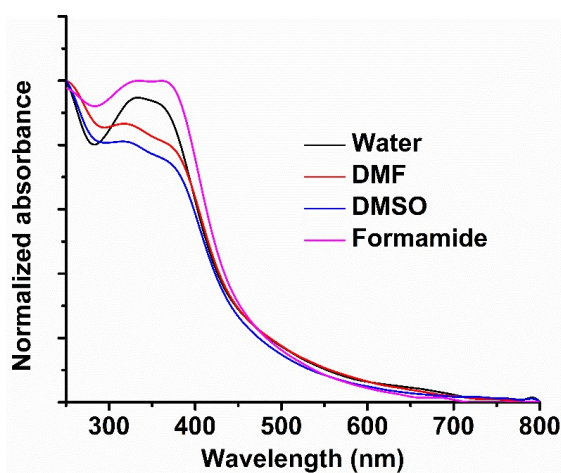


Figure S15. UV-Vis absorption spectra of  $CD_{G-EDA}$  in water, DMF, DMSO and formamide.

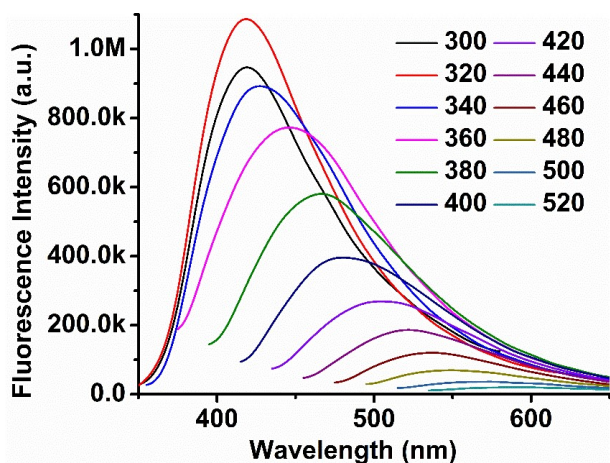


Figure S16. Steady-state fluorescence spectra of  $CD_{G-EDA}$  in water.

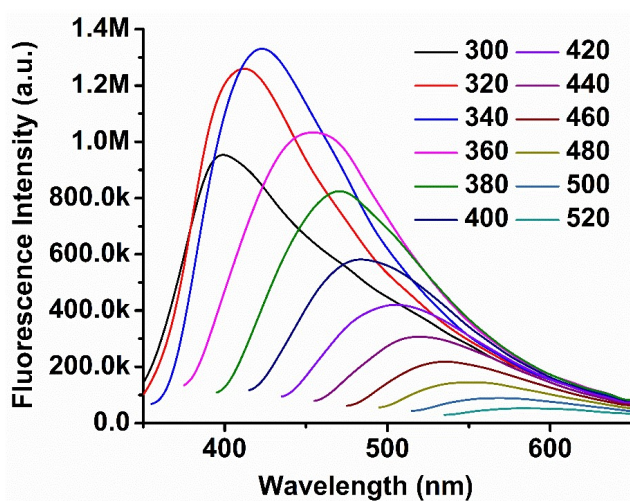


Figure S17. Steady-state fluorescence spectra of  $CD_{G-EDA}$  in DMF.

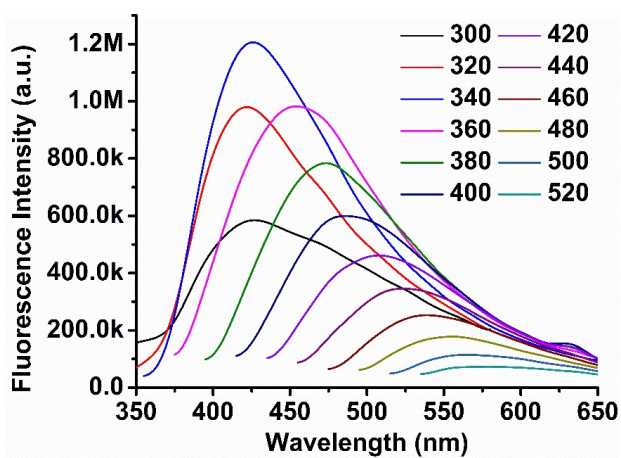
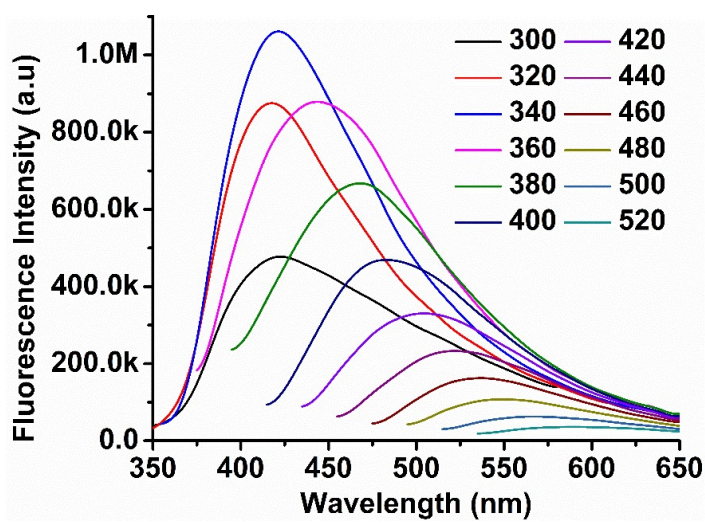
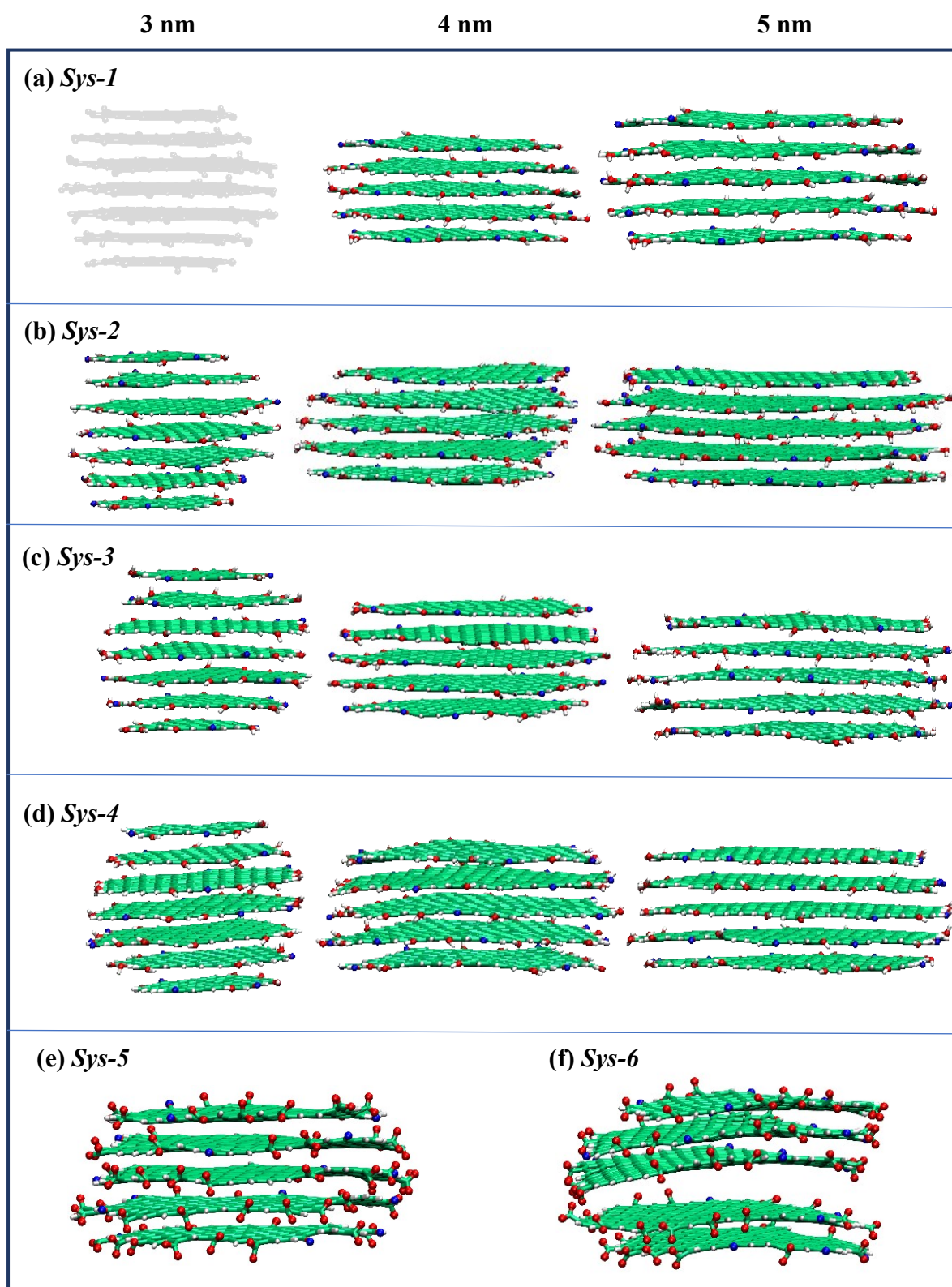


Figure S18. Steady-state fluorescence spectra of  $CD_{G-EDA}$  in DMSO.



**Figure S19.** Steady-state fluorescence spectra of CD<sub>G-EDA</sub> in formamide.



**Figure S20.** Equilibrated snapshots of the CD in all six simulated systems. Different atoms are color coded as carbon (lime green), hydroxyl and carboxyl oxygen (red), carbonyl oxygen (blue), and hydrogen (white).

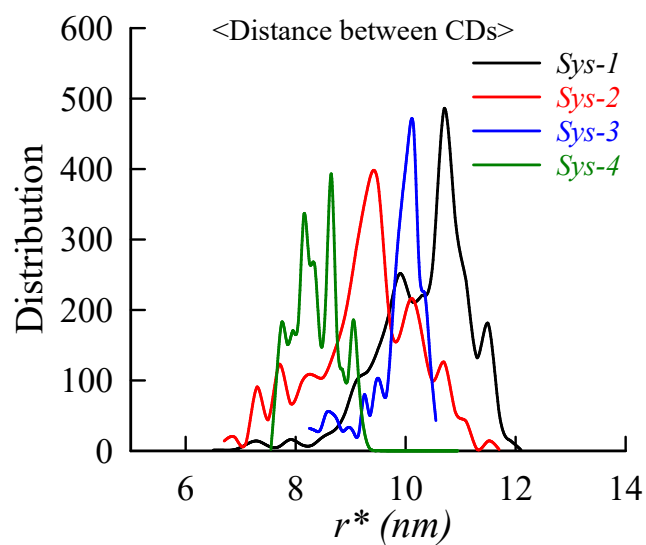


**Figure S21.** Distribution profile for the average distance between the four CDs in four simulated systems. The CDs are placed sufficiently far enough, and no interactions are observed between them throughout the simulation run. This is also visible in the snapshots presented in Figure S3.

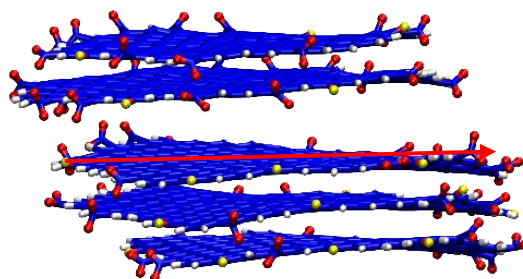


**Figure S22.** The defined vectors connecting the end carbon atoms of the two innermost layers of 3:7 CO: COO<sup>-</sup> CD used for calculating the intramolecular kinetics of CD.

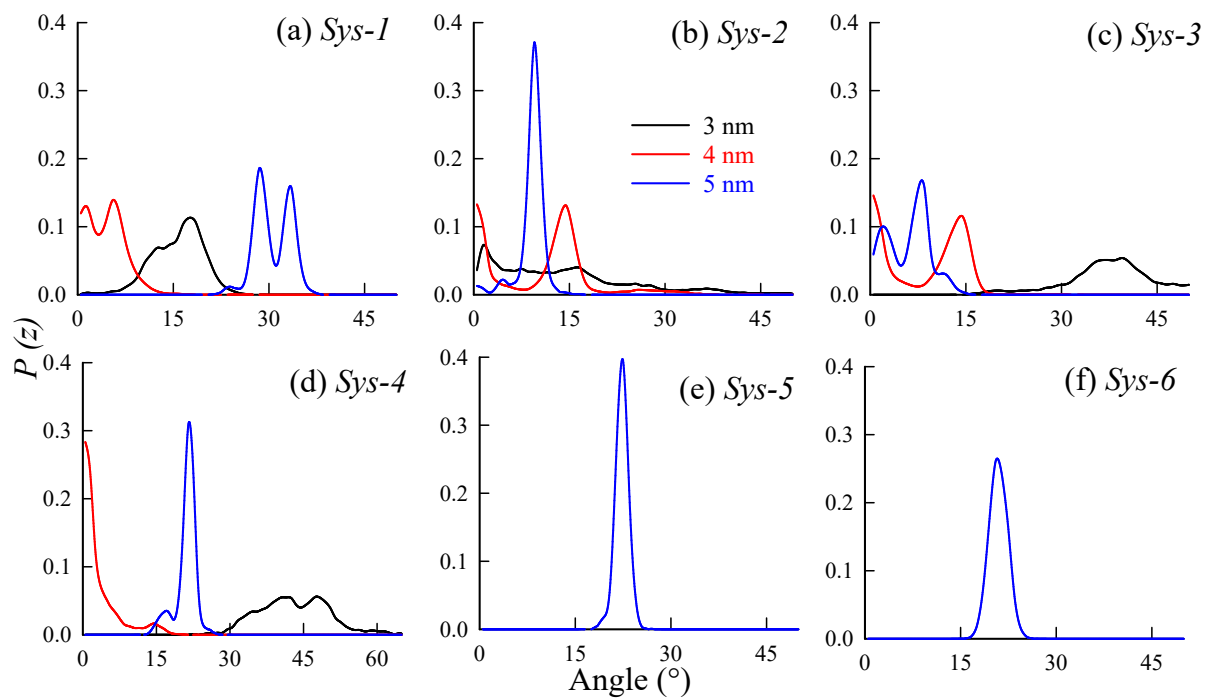


**Figure S23.** The probability distribution of angular orientation profiles calculated between the vector defined for the two innermost layers of the CD in all six simulated systems.

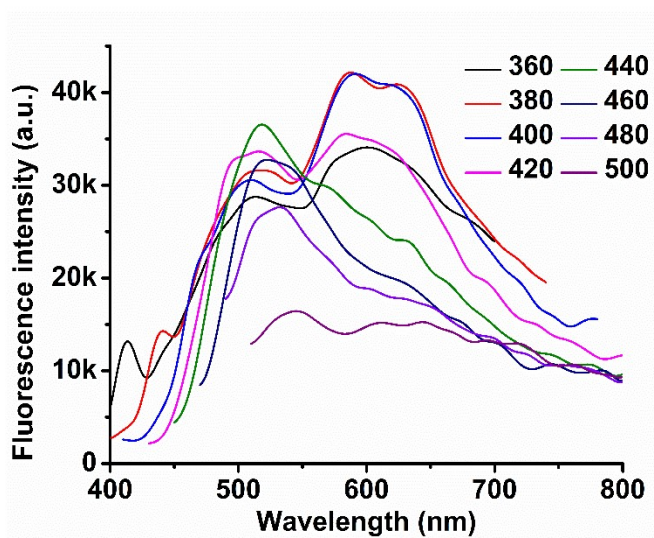


**Figure S24.** Steady-state fluorescence spectra of the P dispersion of CD<sub>ARS-G</sub>.

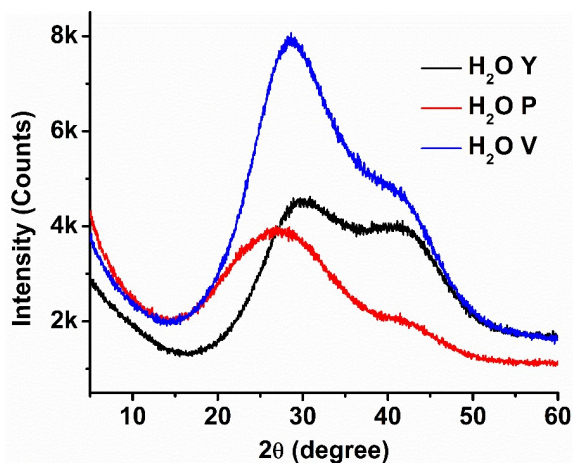


Figure S25. pXRD spectra of the Y, P and V dispersions of  $CD_{ARS-G}$  in water.

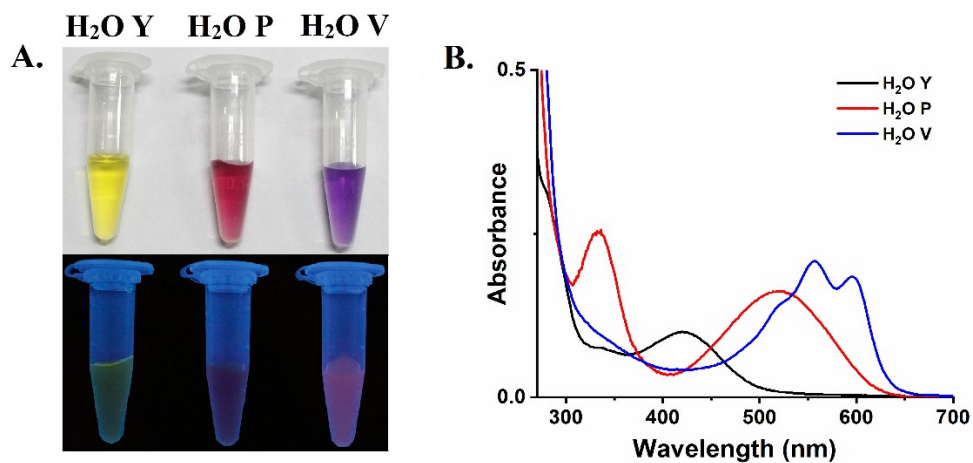


Figure S26. Digital image and UV-Vis absorption spectra of the Y, P, and V dispersions  $CD_{ARS-CA}$ .

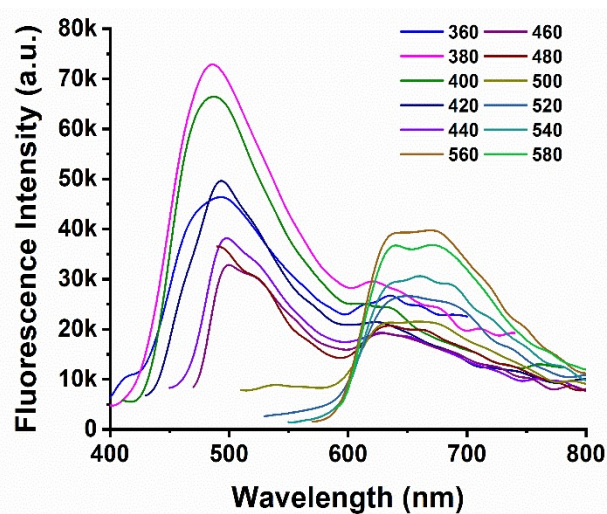
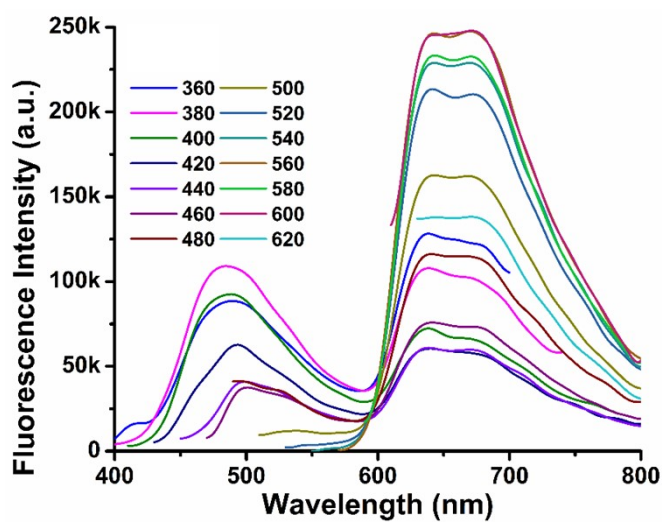
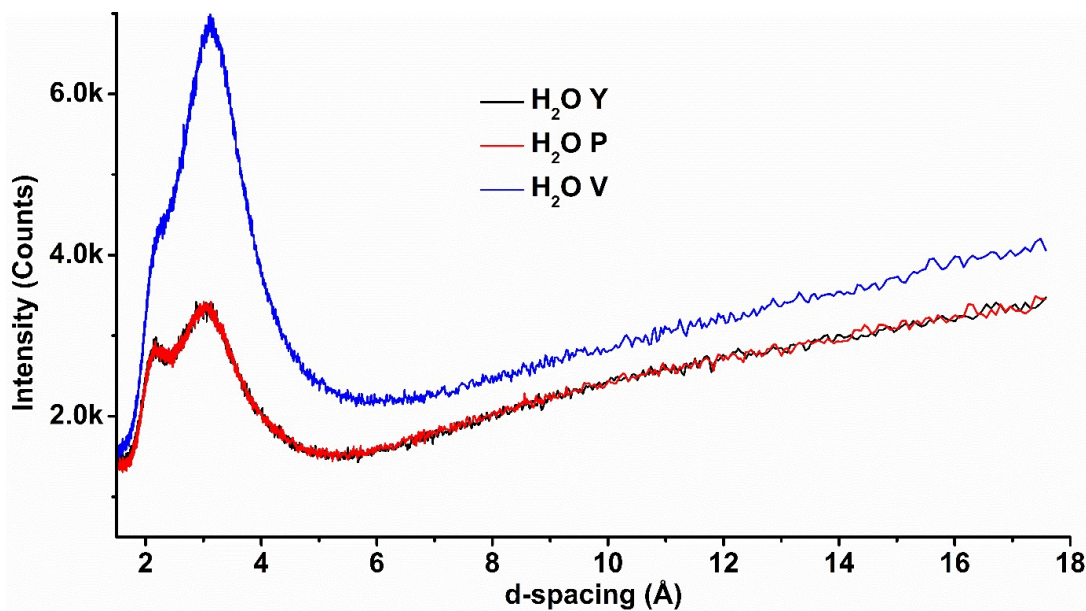


Figure S27. Steady-state fluorescence spectra of the P dispersion of  $CD_{ARS-CA}$ .



**Figure S28.** Steady-state fluorescence spectra of the V dispersion of CD<sub>ARS-CA</sub>.



**Figure S29.** pXRD spectra of the Y, P and V dispersion of CD<sub>ARS-CA</sub> with respect to d-spacing values.

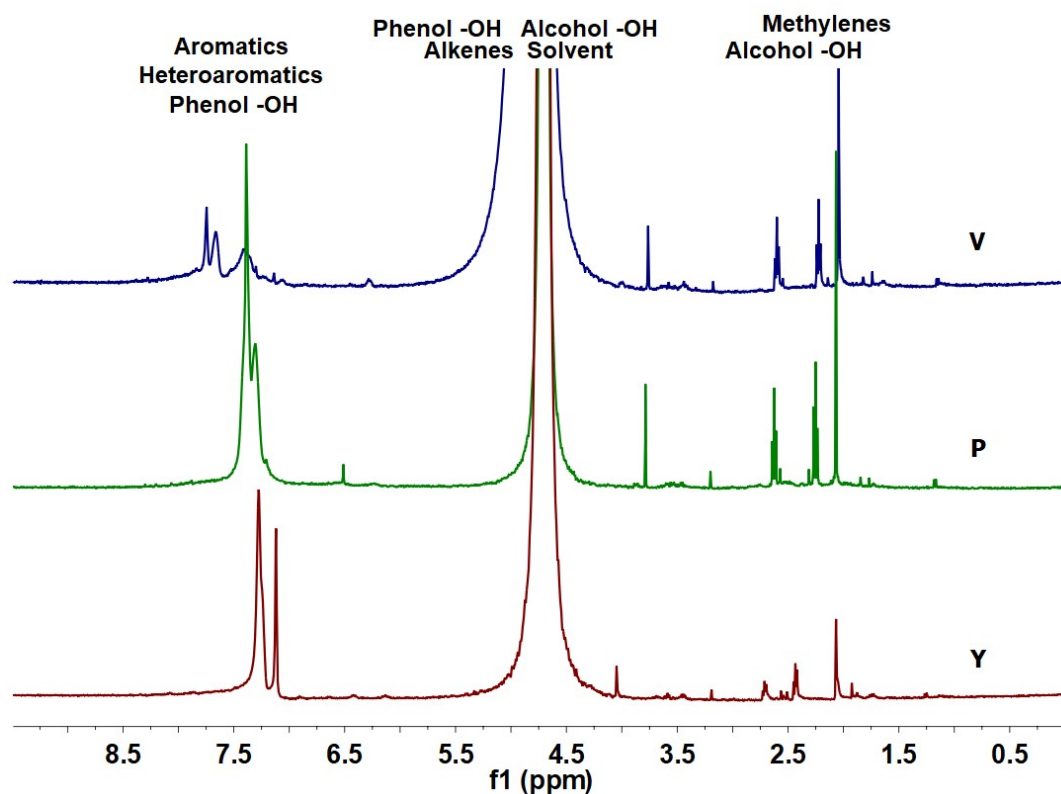


**Figure S30.**  $^1\text{H}$  NMR spectra of the Y, P and V dispersion of  $\text{CD}_{\text{ARS-G}}$  in  $\text{D}_2\text{O}$ .

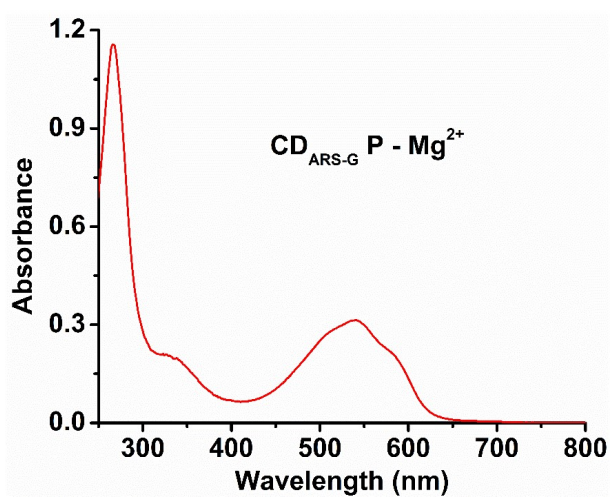


**Figure S31.** UV-Vis absorption spectra of the  $\text{CD}_{\text{ARS-G}}$  water dispersion in presence of  $\text{Mg}^{2+}$  ion at physiological pH.

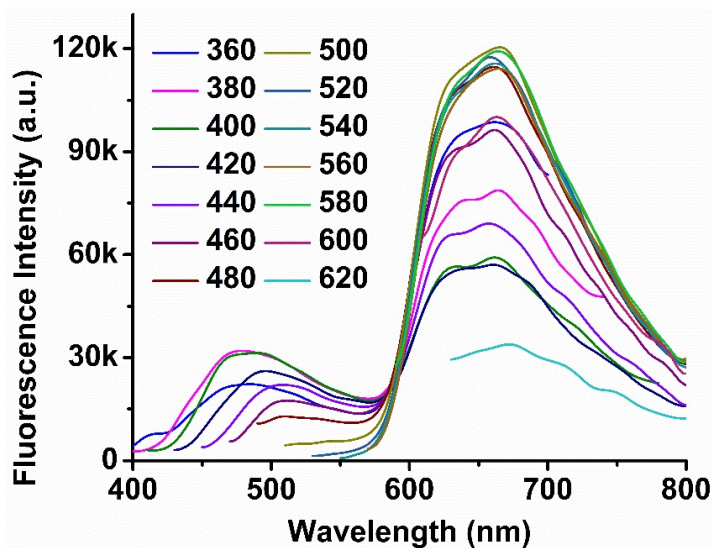


**Figure S32.** Steady-state fluorescence spectra of the  $CD_{ARS-G}$  water dispersion in presence of  $Mg^{2+}$  ion at physiological pH.

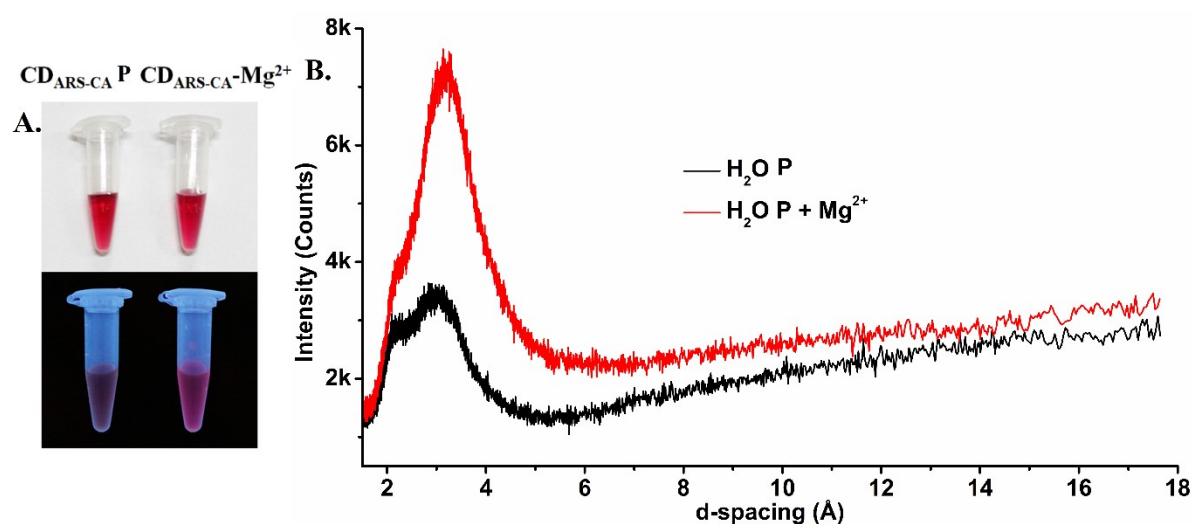


**Figure S33.** A. Digital image, and B. d-spacing distribution of the  $CD_{ARS-CA}$  water dispersion in presence of  $Mg^{2+}$  ion at physiological pH.

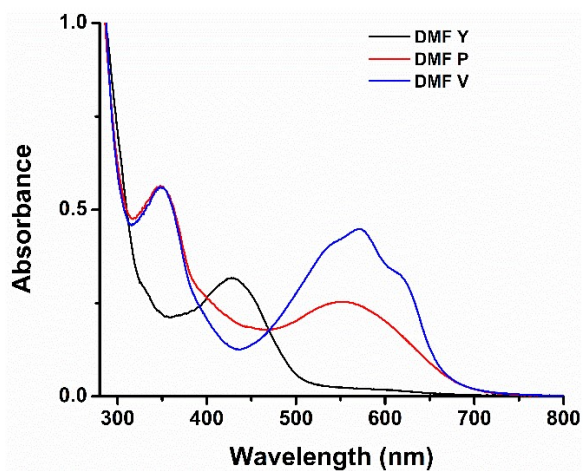


Figure S34. UV-Vis absorption spectra of the CD<sub>ARS-G</sub> Y, P, and V dispersions in DMF.

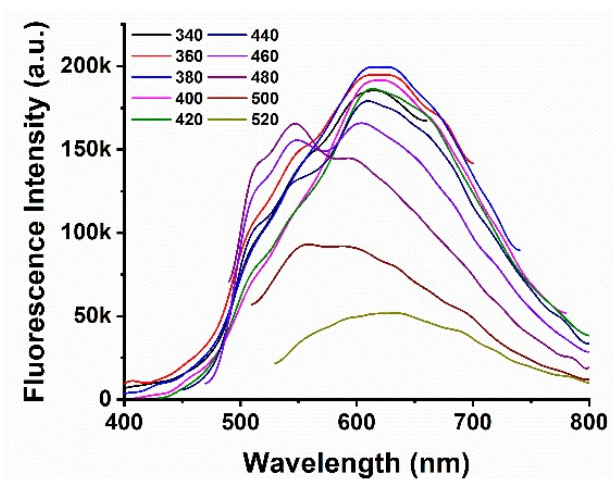


Figure S35. Steady-state fluorescence spectra of the CD<sub>ARS-G</sub> Y dispersion in DMF.

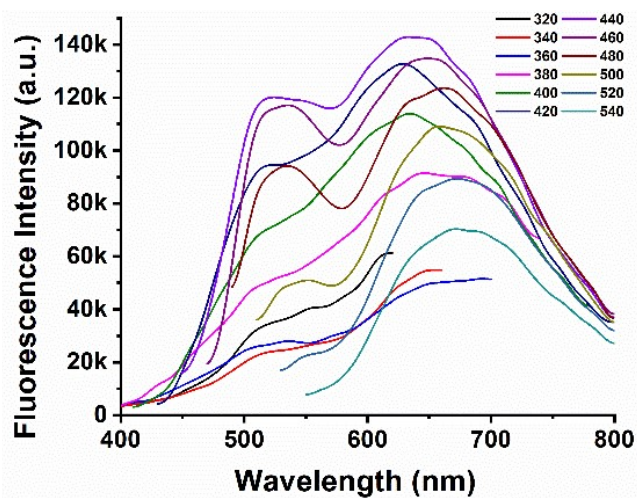
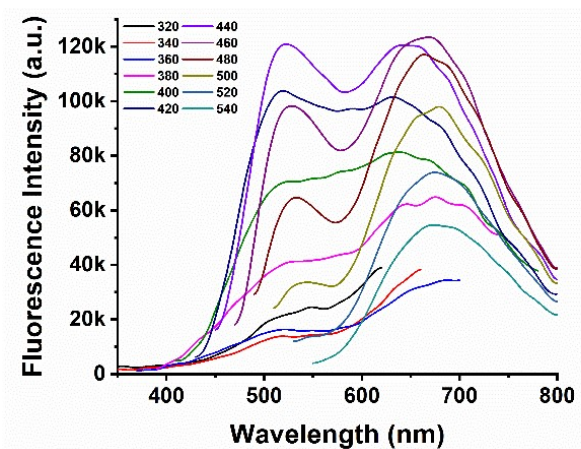
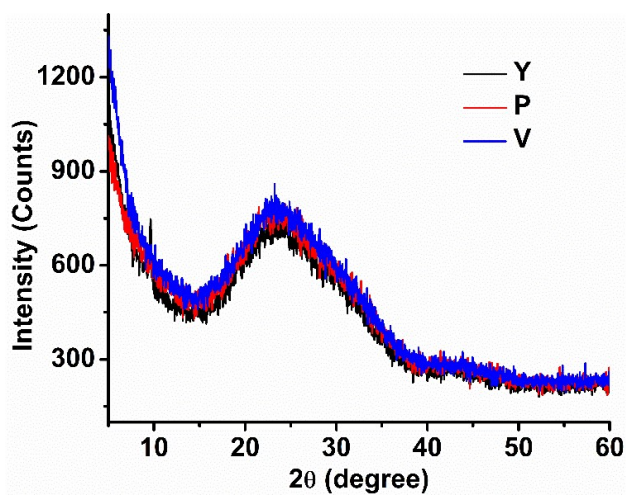


Figure S36. Steady-state fluorescence spectra of the CD<sub>ARS-G</sub> P dispersion in DMF.



**Figure S37.** Steady-state fluorescence spectra of the CD<sub>ARS-G</sub> V dispersion in DMF.



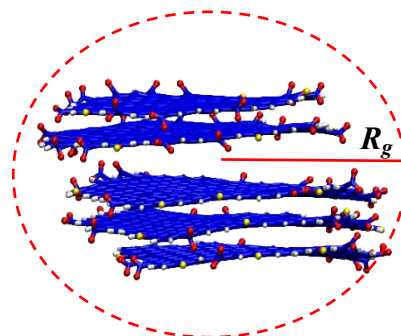
**Figure S38.** pXRD spectra of the Y, P, and V form of CD<sub>ARS-G</sub> in dry state.

**Table S1.** Geometrical details of the four types of CDs modeled in the simulation.

| Edge size | # Layers           |       | Diameter of the central layer (nm) | Dot height (nm) | # Functional groups |     |                   | # Atoms |
|-----------|--------------------|-------|------------------------------------|-----------------|---------------------|-----|-------------------|---------|
|           | above middle layer | total |                                    |                 | -OH                 | -CO | -COO <sup>-</sup> |         |
| 6         | 3                  | 7     | 3                                  | 2               | 57                  | 22  | –                 | 1435    |
| 8         | 2                  | 5     | 4                                  | 1.5             | 58                  | 25  | –                 | 2051    |
| 10        | 2                  | 5     | 5                                  | 1.5             | 71                  | 33  | –                 | 3164    |
| 8         | 2                  | 5     | 4                                  | 1.5             | –                   | 24  | 56                | 2080    |

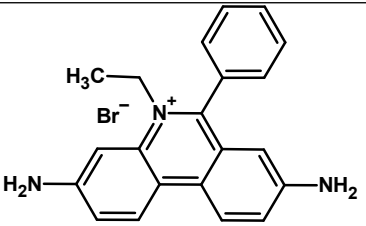
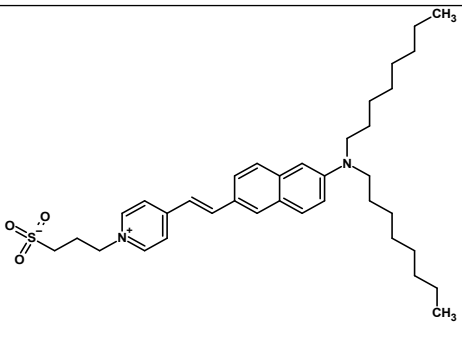
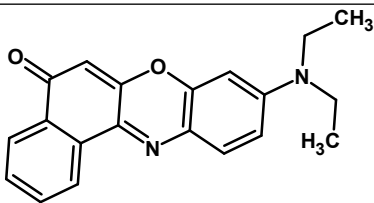
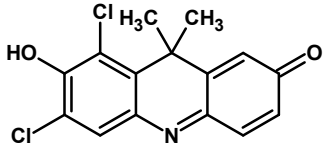
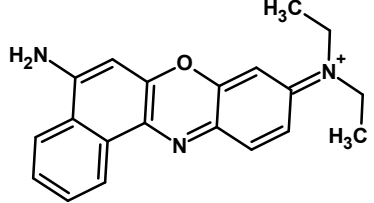
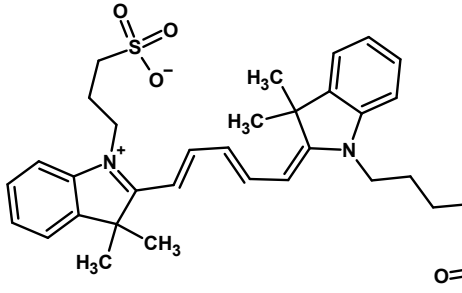
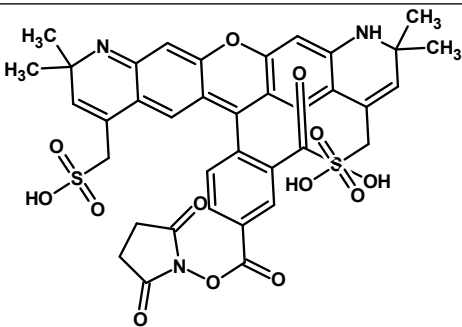
**Table S2.** Radius of gyration ( $R_g$ ) of CDs solvated in different solvents.

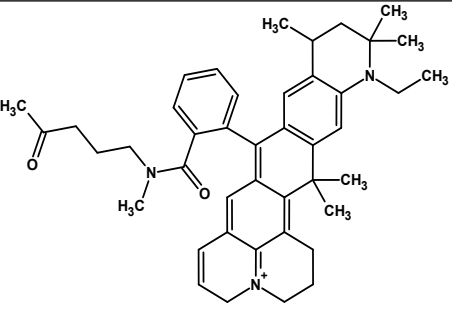
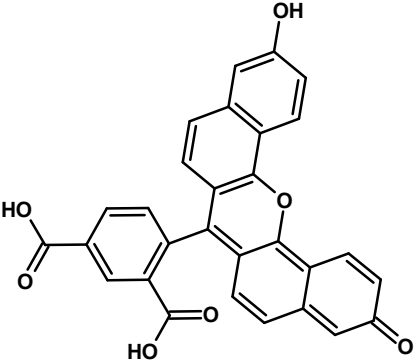
| Solvent      | $R_g$ (nm) |      |      |
|--------------|------------|------|------|
|              | 3 nm       | 4 nm | 5 nm |
| <i>Sys-1</i> | 1.08       | 1.33 | 1.62 |
| <i>Sys-2</i> | 1.08       | 1.33 | 1.62 |
| <i>Sys-3</i> | 1.08       | 1.33 | 1.62 |
| <i>Sys-4</i> | 1.08       | 1.33 | 1.62 |
| <i>Sys-5</i> | -          | 1.50 | -    |
| <i>Sys-6</i> | -          | 1.51 | -    |



**Table S3.** Red fluorescent dyes.

| Dye             | Excitation, nm | Emission, nm | Stokes shift, $\text{cm}^{-1}$ | Structure |
|-----------------|----------------|--------------|--------------------------------|-----------|
| MitoTracker Red | 578            | 599          | 606.55                         |           |
| Alexa 568       | 576            | 603          | 777.36                         |           |

|                        |     |     |         |  |
|------------------------|-----|-----|---------|--|
| Ethidium Bromide       | 524 | 605 | 865.31  |    |
| Di-8 ANEPPS            | 469 | 630 | 2555.04 |    |
| Nile Red               | 559 | 637 | 646.65  |    |
| DDAO pH 9.0            | 648 | 657 | 658.13  |   |
| Nile Blue, EtOH        | 631 | 660 | 5448.95 |  |
| Cy 5                   | 646 | 664 | 2190.50 |  |
| BODIPY 650/665-X, MeOH | 646 | 664 | 211.40  |  |

|   |     |     |        |   |
|---|-----|-----|--------|---|
| Atto 647                                  | 644 | 670 | 209.47 |  <p>The chemical structure of Atto 647 is a complex polycyclic molecule. It features a central benzoxazine ring system. Attached to this system are a phenyl ring, a pyridinium ring (with a positive charge on the nitrogen atom), and a piperidine ring. The piperidine ring is substituted with two methyl groups and an ethyl group. A side chain consisting of a propyl group and a methyl group is attached to the nitrogen atom of the piperidine ring. The overall structure is highly branched and contains several heterocyclic rings.</p>                              |
| Carboxynapht<br>hofluorescein,<br>pH 10.0 | 600 | 674 | 696.35 |  <p>The chemical structure of Carboxynapht hofluorescein at pH 10.0 is a complex polycyclic molecule. It features a central benzoxazine ring system. Attached to this system are a phenyl ring, a pyridinium ring (with a positive charge on the nitrogen atom), and a piperidine ring. The piperidine ring is substituted with two methyl groups and an ethyl group. A side chain consisting of a propyl group and a methyl group is attached to the nitrogen atom of the piperidine ring. The overall structure is highly branched and contains several heterocyclic rings.</p> |